Study of Energy Migration and Trapping in a Poly(ethylene 2,6-naphthalenedicarboxylate) Matrix by Fluorescence Spectroscopy

Jean Duhamel*

Institute for Polymer Research, Department of Chemistry and Biochemistry, University of Waterloo, Waterloo, ON N2L 3G1, Canada

Allan S. Jones and Todd J. Dickson

Eastman Chemical Company, Research Laboratories, Kingsport, Tennessee 37662

Received March 28, 2000; Revised Manuscript Received June 5, 2000

ABSTRACT: The efficiency of dimethyl iodoterephthalate (I-DMT), 2,6-dimethyl 1-benzoylnaphthalate (BZN), and 2,6-bis(2-hydroxyethylthio)naphthalene (NSEG) at quenching the fluorescence of the poly(ethylene 2,6-naphthalenedicarboxylate) (PEN) matrix has been investigated by steady-state and time-resolved fluorescence spectroscopy. All three quenchers are capable of capturing the energy migrating between naphthalene dimers. Steady-state fluorescence data indicate that, after the quencher has trapped the migrating energy, the excited quencher can relax either via nonradiative processes (I-DMT) or via radiative processes (BZN and NSEG). Fluorescence decay measurements show that NSEG quenches PEN fluorescence best, followed by BZN, and I-DMT is the worst quencher. Quenching efficiency of a given quencher increases linearly with quencher concentration, for quencher contents below the overlap concentration, for which the entire polymer matrix is covered by quenchers. Above the overlap concentration, quenching efficiency increases at a slower pace because any additional quencher quenches an already quenched volume. Our experimental results could be interpreted by compartmentalizing the quenching process in the polymer matrix. Compartmentalization could be handled by a blob model, which was applied to quantify the quenching efficiency of I-DMT and BZN.

Introduction

Poly(ethylene 2,6-naphthalenedicarboxylate) (PEN) exhibits higher oxygen and carbon dioxide barrier properties, higher glass transition temperature, higher melt temperature, higher tensile strength, and a higher modulus than poly(ethylene terephthalate) (PET). These features make it a desirable material for certain packaging applications, were it not for PEN's strong bluish fluorescence, which arises from the naphthalene moieties constituting the polymer matrix. PEN's inherent fluorescence yields products with unappealing appearance, a serious drawback for a material destined for packaging applications.[1]

This problem led to several studies aimed at better understanding the photophysical processes taking place inside the PEN matrix.[1−5] Over the years, it was determined that, in the bulk, PEN is made of naphthalene monomers and ground-state (GS) dimers. Excitation of the PEN matrix results in the formation of excited monomers and dimers. The energy can migrate between monomers, between dimers, and can be transferred from an excited monomer to a GS dimer. However, the back-reaction involving the transfer of energy from an excited dimer to a ground-state monomer is expected to be the least favorable of all photophysical processes.[2]

Although energy migration between naphthalene monomers and GS dimers can be looked at as a serious complication for a careful photophysical study of PEN, it is a very advantageous feature when the objective is to reduce fluorescence. As a matter of fact, it is expected that the insertion of a nonfluorescent (NF) quencher in the PEN matrix will intercept the migrating excitation before it can find a PEN fluorescent trap (typically a naphthalene GS dimer), resulting in more efficient quenching. The quencher would play the same role as a reaction center in plants.[6] As in plants where energy migrates between chlorophyll pigments until a reaction center is encountered, the energy would migrate inside the PEN matrix until the inserted NF quencher would be encountered. This effect has been coined the antenna effect.[7]

Three quenchers were considered in this study. They were dimethyl iodoterephthalate (I-DMT), 2,6-dimethyl 1-benzoylnaphthalate (BZN), and 2,6-bis(2-hydroxyethylthio)naphthalene (NSEG). These quenchers were copolymerized with dimethyl 2,6-naphthalenedicarboxylate and ethylene glycol. These molecules contain elements, such as iodine, benzoyl, and sulfur, which can absorb the excess energy of the excited species and relax to their GS level via nonradiative processes.[8] The photophysical properties of the copolymer matrices were investigated by steady-state and time-resolved fluorescence.

Theories have been developed which characterize the process of energy migration.[9−12] They usually consider a single species of donors (D) among which energy hops, until a trap (T) is encountered. Energy migration and trapping are assumed to occur via energy transfer. The efficiency of energy transfer is characterized by the Forster radius R_0, which is estimated by determining the overlap between the absorption spectrum of the acceptor and the emission spectrum of the donor.[13] In the case of energy migration, the acceptor is the same molecule as the donor and the Forster radius between two donors (R_0^{DD}) is obtained. In the case of trapping, the acceptor is a different molecule, and the Forster radius between the donor and the trap (R_0^{DT}) is ob-

* To whom correspondence should be addressed.

10.1021/ma0005419 CCC: $19.00
Published on Web 07/27/2000

tained. Unfortunately, the R_0 parameter is difficult to determine for solid-state samples, especially for PEN for which the concentration of donors (essentially the GS dimers) is quasi-impossible to estimate. In any approach, the values of R_0^{DD} and R_0^{DT} would have to be either assumed or retrieved as the parameters of the analysis software.

The system under scrutiny, PEN, is constituted of two donor species instead of the single one usually considered for theoretical work,[9−12] namely the naphthalene monomers and GS dimers. However, upon addition of 1 mol % of the quenchers I-DMT, BZN, and NSEG, the contribution arising from the monomers was found to disappear so that PEN can be considered to be made of a single donor species, namely the naphthalene dimers. Energy migration occurs between the naphthalene dimers until trapping takes place between an excited naphthalene dimer and the quencher. The best quencher of the fluorescence emitted by the PEN matrix was found to be NSEG, the next best one was BZN, and the worst one was I-DMT. Their respective quenching efficiencies were quantified by using a blob model.

Experimental Section

Melt Polymerizations. Ethylene glycol, dimethyl terephthalate (DMT), I-DMT, BZN, and NSEG were obtained from Eastman, and dimethyl-2,6-naphthalene dicarboxylate (DMN) was obtained from Amoco Chemicals. They were used without further purification. The appropriate amounts of starting materials were charged into a 500 mL one-neck round-bottom flask, along with catalyst metals, and polymerized under conditions similar to those previously reported.[1] Two polymer matrices were considered in this study. One contained 25 mol % of DMN and 75 mol % of DMT (referred to as T25N2 in this report), and the other was pure PEN made of 100 mol % DMN. Addition of I-DMT, BZN, and NSEG to the reaction mixtures yielded polymer matrices with the required quencher concentration. The polymers were allowed to slowly cool at 23 °C before isolation, yielding polymers with various levels of crystallinity for T25N2, PEN, and copolymers with quencher concentrations in T25N2 and PEN ranging from 0.5 to 10 mol %.

Sample Preparation. Samples of each polymer were micropulverized in a lab grinder into a fine powder and sieved through a 120 mesh screen (hole size 0.0049 in.). The powders were then introduced into a 1 cm square quartz fluorescence cell, and fluorescence measurements were performed on the solid-state samples without degassing.

Steady-State and Time-Resolved Fluorescence Measurements. All fluorescence measurements were acquired on a Photon Technology International, Inc., spectrofluorometer. Fluorescence excitation and emission spectra used a xenon-arc lamp for excitation. For the time-resolved fluorescence measurements, excitation was provided by a hydrogen-filled flash lamp. All powdered samples were studied in the front-face configuration. Before acquisition of any fluorescence decay, an instrument response was collected at the excitation wavelength. The usual conditions to study the fluorescence of the polymer samples were $\lambda_{ex} = 350$ nm and $\lambda_{em} = 480$ nm to monitor the naphthalene excited dimer. Times per channel of 0.191 and 0.382 ns/channel over 512 channels were used depending on the quencher content and its quenching efficiency. All decays held a minimum of 10 000 counts at the decay maximum. The fluorescence decays were fitted with either a sum of exponentials according to eq 1 with k equal to 2 or 3 or a stretched exponential given in eq 10. The fitting software corrected for the presence of light scattering in the decays.[14]

$$f(t) = \sum_{i=1}^{k} A_i \exp(-t/\tau_i) \tag{1}$$

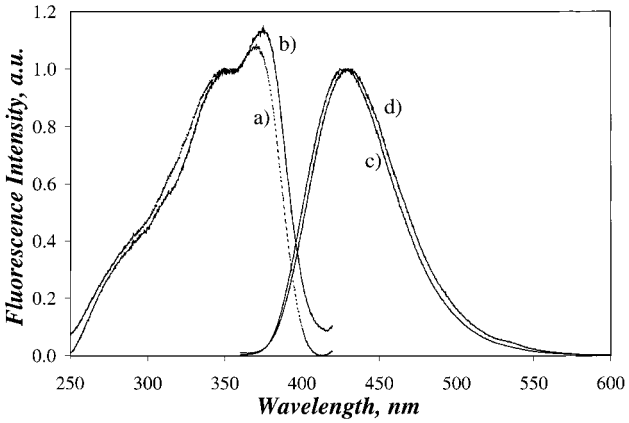

Figure 1. Steady-state excitation spectra of (a) PEN and (b) PEN with 7 mol % of I-DMT and steady-state emission spectra of (c) PEN and (d) PEN with 7 mol % of I-DMT. The excitation spectra are obtained with an emission wavelength fixed at 430 nm. The fluorescence emission spectra were obtained with a 350 nm excitation wavelength.

The parameters of the fits were optimized by using the Marquardt−Levenberg algorithm.[15] The quality of the fits was estimated from the χ^2, the residuals, and the autocorrelation function of the residuals. The average decay time $\langle\tau\rangle$ was calculated from eq 2:

$$\langle\tau\rangle = \frac{\sum_{i=1}^{k} A_i\tau_i}{\sum_{i=1}^{k} A_i} \tag{2}$$

Simulation of Fluorescence Decays. Fluorescence decays were simulated according to the theory developed by Loring et al.,[9] which is hereafter referred to as the LAF theory. According to the LAF theory, the Laplace transform of the probability ($\tilde{G}_{DT}(0,\epsilon)$) that an excitation is somewhere in the donor ensemble is given by

$$\tilde{G}_{DT}(0,\epsilon) = \frac{[\tilde{G}^S(\epsilon)]^2}{\tilde{G}^S(\epsilon) - \tilde{\Delta}[0,\tilde{G}^S(\epsilon)]} \tag{3}$$

where the functions $\tilde{G}^S(\epsilon)$ and $\tilde{\Delta}[0,\tilde{G}^S(\epsilon)]$ have been determined by Loring et al.[9] Equation 3 was then back-transformed into the real space using a standard procedure to yield $G_{DT}(t)$.[16] The fluorescence decays ($F_D(t)$) of the excited donor undergoing energy migration and trapping were obtained as shown in eq 4

$$F_D(t) = e^{-t/\tau_D} G_{DT}(t) \tag{4}$$

where τ_D is the donor lifetime. Poisson noise was added to the resulting fluorescence decays,[17] which were fitted with a triexponential function.

Results

For all copolymer samples, steady-state excitation and emission spectra were taken. Figures 1−3 display the main features of these spectra. PEN excitation and emission spectra are used as reference and are shown in all figures. The excitation spectra were normalized at 350 nm. They were obtained with a 430 nm emission wavelength. The emission spectra were normalized at their maximum. They were obtained with a 350 nm excitation wavelength.

The PEN excitation spectrum is broad and exhibits two maxima at 347 and 370 nm. Upon insertion of 7

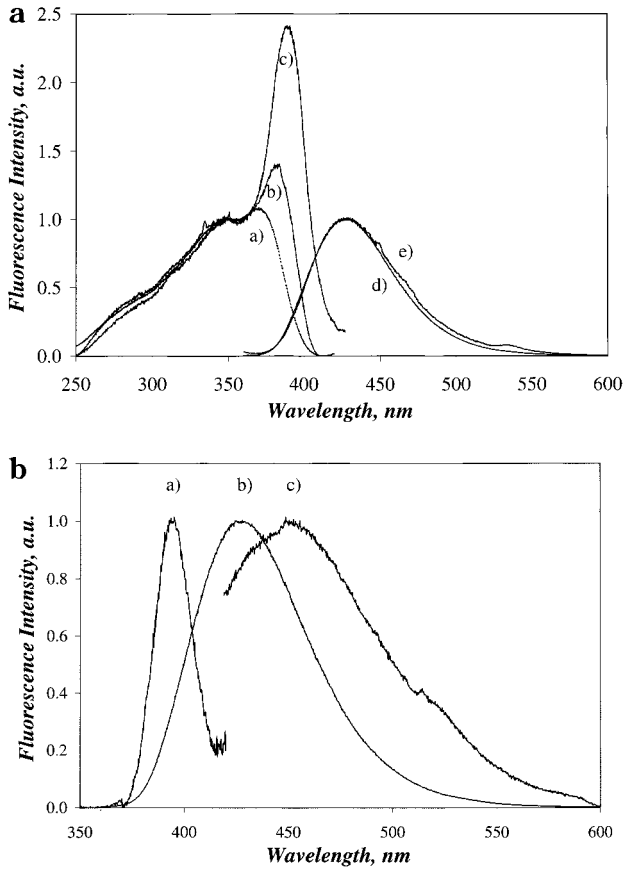

Figure 2. (a) Steady-state excitation spectra of (a) PEN and (b) PEN with 3 mol % of BZN and (c) PEN with 10 mol % of BZN and steady-state emission spectra of (d) PEN and (e) PEN with 10 mol % of BZN. The excitation spectra are obtained with an emission wavelength fixed at 430 nm. The fluorescence emission spectra were obtained with a 350 nm excitation wavelength. (b) Steady-state excitation spectrum of (a) poly-BZN (obtained with an emission wavelength fixed at 430 nm) and steady-state emission spectra of (b) PEN (obtained with a 350 nm excitation wavelength) and (c) polyBZN (obtained with a 390 nm excitation wavelength).

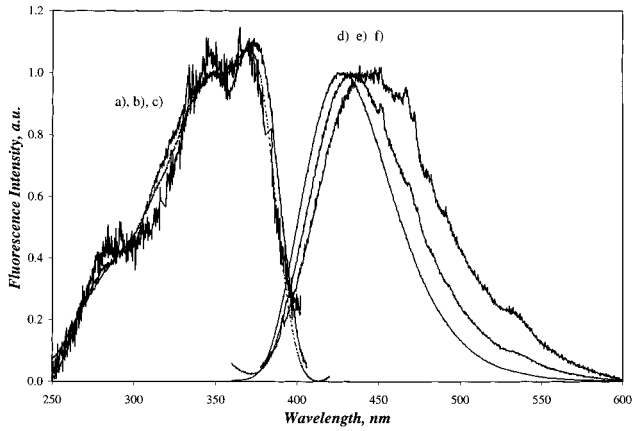

Figure 3. Steady-state excitation spectra of (a) PEN and (b) PEN with 1 mol % of NSEG and (c) PEN with 5 mol % NSEG and steady-state emission spectra of (d) PEN, (e) PEN with 1 mol % NSEG, and (f) PEN with 5 mol % of NSEG. The excitation spectra are obtained with an emission wavelength fixed at 430 nm. The fluorescence emission spectra were obtained with a 350 nm excitation wavelength. The noise in the spectra results from the high quenching efficiency of NSEG.

mol % of I-DMT in the PEN matrix, the overall features of the excitation and emission spectra are preserved with respect to PEN, as shown in Figure 1. The excitation peak at 370 nm shifts slightly to the right and increases slightly in intensity. The emission maximum shifts from 427 to 431 nm, a small change considering how broad these spectra are, and the fact that these samples are solid-state samples, which are observed with a front-face geometry. These small spectral alterations could not be detected for polymer matrices with I-DMT contents smaller than 5 mol %.

Figure 2a presents similar data using BZN as a quencher. The features of the excitation spectra are preserved with respect to the PEN reference for wavelengths shorter than 365 nm. However, addition of BZN has a strong effect on the excitation spectra for wavelengths larger than 365 nm. An excitation band located at 390 nm appears, and its intensity increases linearly with increasing amounts of BZN. The emission spectrum of PEN with BZN is hardly affected by the presence of a strong absorption band at 390 nm, and it overlaps the fluorescence of pure PEN. The emission maximum of all BZN-containing PEN samples was located at the same position. To investigate the broad band, which appears at 390 nm upon addition of BZN to the PEN matrices, a sample of poly(BZN) was prepared. Its excitation spectrum showed no signal for wavelengths smaller than 365 nm, but the signal increases for wavelengths larger than 365 nm and peaks at 395 nm (cf. Figure 2b), confirming the observations made for the PEN samples containing BZN. When poly(BZN) was excited at 390 nm, a broad structureless fluorescence emission appeared with a maximum at 455 nm. The fluorescence emission of poly(BZN) was shifted to higher wavelengths when compared to that of PEN. This wavelength shift was not observed for any of the BZN-containing PEN samples studied in this report.

NSEG turned out to be the most efficient PEN quencher which was tested in this study. The polymer matrix had a fluorescence intensity, which was reduced strongly upon introduction of NSEG, which explains the noise in the data presented in Figure 3. The excitation spectra of the PEN matrices were very similar whether NSEG was present or not, as shown in Figure 3. The emission maximum shifted continuously with NSEG content from 427 nm for pure PEN to 445 nm for a PEN matrix with 5 mol % of NSEG.

Fluorescence decay measurements are better suited than steady-state fluorescence measurements to establish the quenching efficiency of a given quencher. This is due to the fact that some of the quenchers have an absorption spectrum, which overlaps with the excitation wavelength and also with the fluorescence emission of pure PEN. Thus, a reduction in the emission intensity observed by steady-state fluorescence could be due to the quenchers blocking the excitation of the polymer matrix or/and the PEN emission via reabsorption. However, true quenching will be observed by time-resolved fluorescence as a shortening of the fluorescence decays, as long as the quenching is not static. Consequently, fluorescence decays were taken for all copolymer samples. The samples were excited at 350 nm, and the emission was monitored at 480 nm. Figure 4 shows the fluorescence decays of PEN matrices loaded with increasing amounts of BZN. After a short rise time, pure PEN is almost monoexponential with a decaytime of 26.5 ns. Addition of BZN to the copolymer matrix results in a shortening of the fluorescence decays, indicating quenching. The decays were fitted with a sum of three

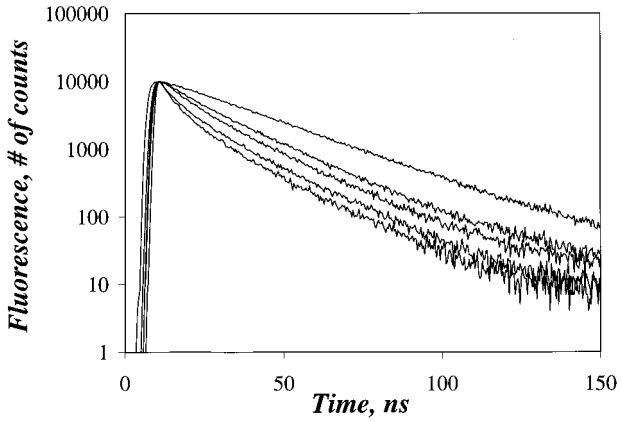

Figure 4. Fluorescence decays of PEN with BZN contents ranging from 0 mol % (pure PEN, top decay) to 1, 2, 4, 5, and 10 mol % (bottom decay). The fluorescence decays were acquired by exciting the sample at 350 nm and monitoring the emission at 480 nm. The time per channel was 0.382 ns/channel.

exponentials, fixing the third decay time to equal 26.5 ns, the lifetime of PEN excited dimers.[2] The preexponential factors and the decay times obtained from this analysis are listed in Table 1. Addition of each quencher to the PEN matrix led to fluorescence decays with a strongly nonexponential character. For all three quenchers, the contribution of the long decay time fixed to equal 26.5 ns in the analysis decreases with quencher content down to barely detectable levels at high quencher content. This indicates that at high quencher concentrations all excited naphthalene dimers are affected by the presence of the quencher inside the polymer matrix.

Addition of 1 mol % of I-DMT, BZN, and NSEG results in PEN fluorescence decays which exhibit no rise time. As mentioned previously,[2] the fluorescence emitted by PEN at 480 nm is due to GS dimers, which are excited either directly or indirectly after the energy, first migrates among naphthalene monomers, second is transferred to GS dimers, and third migrates among GS dimers until it reaches a GS dimer trap. The rise time, which is observed in pure PEN, reflects the time taken by the excitation to reach a ground-state dimer trap by energy migration. Since addition of very small amounts of quencher (1 mol %) is enough to suppress this rise time, it indicates that these quenchers are very efficient at intercepting the energy while it still migrates among naphthalene monomers. Much larger loads of quencher are required to quench the fluorescence of the GS dimers. This effect could arise from the fact that the average distance between naphthalene monomers is larger than the average distance between GS dimers. In the PEN matrix, large pools of naphthalene GS dimers separate naphthalene monomers. Energy migration between monomers should occur over distances which are larger than between GS dimers, which are packed together. This feature of the PEN matrix gives the quenchers a better chance of intercepting the energy migrating among monomers than among GS dimers. This effect could be further tested by monitoring the quenching of naphthalene excited dimers in a copolymer containing 25 mol % of DMN and 75 mol % of DMT (T25N2). Because the naphthalene content of T25N2 is smaller than that of pure PEN, single naphthalene monomers in T25N2 can be isolated without being as far as they are in PEN, so that the average distance separating two single naphthalene monomers is smaller in T25N2 than in PEN. It was shown that the fluorescence decay of the naphthalene dimers inside the pure T25N2 matrix does indeed exhibit a more pronounced rise time.[2] Thus, energy migration between monomers is more efficient, and it will take a longer time before the energy is transferred from an excited monomer to a GS dimer. Consequently, a quencher in T25N2 has a smaller chance to intercept the energy migrating between naphthalene monomers. This is actually observed since more than 2 mol % of I-DMT is required to suppress the rise time observed in T25N2, compared to less than 1 mol % in PEN (cf. Table 1a).

The average decay time ($\langle\tau\rangle$) of all fluorescence decays was calculated, and the ratio $\tau_D/\langle\tau\rangle$ was taken as a measure of the quencher efficiency. τ_D is the lifetime of excited naphthalene dimers and is taken to equal 26.5 ns.[2] A plot of $\tau_D/\langle\tau\rangle$ versus the quencher content in the polymer matrix is given in Figure 5. At a given quencher content, the largest $\tau_D/\langle\tau\rangle$ values are obtained with the sequence

$$\frac{\tau_D}{\langle\tau\rangle}(\text{I-DMT}) < \frac{\tau_D}{\langle\tau\rangle}(\text{BZN}) < \frac{\tau_D}{\langle\tau\rangle}(\text{NSEG}) \qquad (5)$$

Thus, NSEG is the best quencher tried in this study. After energy migration between naphthalene monomers has been neutralized in the T25N2 matrix, it is interesting to note that quencher contents of 4 mol % of I-DMT and 4 mol % BZN yield the same $\tau_D/\langle\tau\rangle$ ratio in T25N2 as in PEN (cf. Figure 5). This result indicates that the pools of GS dimers have the same nature in T25N2 and PEN, since the same quencher content in both polymer matrices results in the same quenching efficiency of the excited naphthalene dimers.

In Figure 5 the ratios $\tau_D/\langle\tau\rangle$ are used as a representation of the quencher efficiency. For I-DMT, the ratio $\tau_D/\langle\tau\rangle$ increases linearly with I-DMT content, but for BZN and NSEG, the ratio $\tau_D/\langle\tau\rangle$ exhibits a well-defined break point at or below 1 mol % for NSEG and at 2 mol % for BZN. The presence of these break points will be investigated in more details in the Discussion section. The quenching efficiencies of the quenchers can be attributed to at least two distinct quenching processes. Disappearance of the rise time in the PEN fluorescence decays and strong reduction of the PEN fluorescence are indications that all three quenchers I-DMT, BZN, and NSEG are efficient at capturing the energy migrating inside the PEN matrix. How the now excited quencher releases its excess energy varies depending on the type of quencher. For I-DMT, the steady-state excitation and emission spectra are hardly altered upon addition of I-DMT to the PEN matrix (cf. Figure 1), at least for the quencher contents used in this study. In a PEN matrix, excited I-DMT molecules seem to go down to their ground state according to a nonradiative process. In a PEN matrix, BZN absorbs energy around 390 nm (cf. Figure 2). BZN cannot be excited directly in our fluorescence experiments ($\lambda_{ex} = 350$ nm), because it does not absorb light below 365 nm. However, the BZN excitation spectrum overlaps the emission spectrum of PEN so that energy transfer can occur from a directly excited naphthalene monomer or dimer to a GS BZN. The excited BZN could either go down to its ground state via a nonradiative process or emit fluorescence with a lifetime shorter than τ_D (=26.5 ns), leading to an increased quenching of the PEN matrix. Both processes contribute to the shortening of $\langle\tau\rangle$ for the BZN-containing PEN matrices.

Table 1. Parameters Recovered from the Triexponential Fit of the Fluorescence Decays (λ_{ex} = 350 nm and λ_{em} = 480 nm) of T25N2 and PEN Matrices Containing I-DMT, BZN, and NSEG Using Eq 1

	[Q], mol %	A_1	τ_1, ns	A_2	τ_2, ns	A_3	τ_3, ns	χ^2
				PEN Containing I-DMT				
PEN matrices	1			0.49	17	0.51	26.5	1.24
	2	0.14	7.7	0.61	15.9	0.26	26.5	1.37
	3[a]	0.28	9.1	0.72	21.7			1.50
	4	0.24	6.3	0.56	16.4	0.20	26.5	1.15
	5	0.19	3.9	0.60	13.8	0.21	26.5	1.17
	7	0.44	5.9	0.48	16.9	0.07	26.5	1.27
T25N2 matrices	1	−0.50	2.2	0.38	14.3	1.12	26.5	1.41
	2	−0.66	0.7	0.79	13.7	0.86	26.5	1.24
	4	0.24	5.6	0.45	14.9	0.31	26.5	1.08
				PEN Containing BZN				
PEN matrices	0.5			0.63	14.9	0.37	26.5	1.44
	1.0	0.24	5.7	0.55	16.5	0.22	26.5	1.05
	2.0	0.37	4.6	0.49	14.4	0.14	26.5	1.18
	3.0	0.50	6.0	0.45	18.0	0.05	26.5	1.22
	4.0	0.49	3.3	0.43	13.7	0.08	26.5	1.31
	5.0	0.51	4.0	0.4	14.0	0.08	26.5	1.19
	10.0	0.61	3.4	0.34	13.4	0.05	26.5	1.66
T25N2 matrix	4	0.47	2.8	0.35	12.9	0.18	26.5	1.27
				PEN Containing NSEG				
	1.0	0.63	4.0	0.31	13.9	0.06	26.5	1.17
	2.5	0.77	3.5	0.26	12.6	0.03	26.5	1.34
	5.0	0.77	2.7	0.21	8.8	0.02	26.5	1.25

[a] This decay could not be fitted using three exponentials.

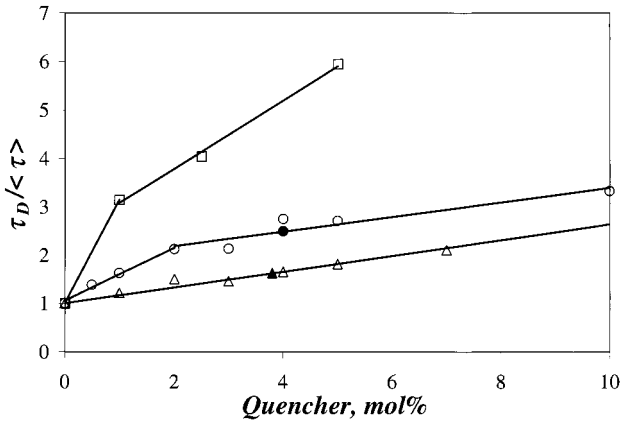

Figure 5. Plot of $\tau_D/\langle\tau\rangle$ as a function of quencher content. The different quencher types are I-DMT (△ in PEN and ▲ in T25N2), BZN (○ in PEN and ● in T25N2), and NSEG (□ in PEN).

The fluorescence of isolated BZN units might be difficult to characterize at the low quencher contents used in this study. This is because no shift in the emission fluorescence spectra could be detected whether a PEN matrix loaded with 5 mol % of BZN was excited at 350 nm (where BZN does not absorb) or at 390 nm (where BZN absorbs). NSEG addition to the PEN matrix results in a strong reduction of the PEN fluorescence and a disappearance of the rise time is observed in the PEN decays. As more NSEG is added, the fluorescence maximum shifts to higher wavelengths. This indicates that NSEG embedded inside the PEN matrix could emit some fluorescence of its own. Upon excitation (either direct or after capture of the migrating energy), NSEG could emit with a shorter lifetime than τ_D (=26.5 ns), resulting in an apparent quenching of the PEN matrix. This behavior would be similar to the one observed for BZN, although NSEG is much more efficient at reducing the PEN emission than BZN is.

Because a significant quenching efficiency is observed for very low contents of all three quenchers considered (as low as 1 mol %) and because the average decay times are substantially shortened, it is impossible that quenching occurs only via simple absorption of the exciting light by the quencher. More plausibly, the energy hops between naphthalene dimers, and it is captured by the quenchers via either an electron- or an energy-transfer mechanism. Once excited, the quencher will either release its energy as heat (I-DMT) or emit a photon and fluoresce with a lifetime shorter than τ_D (BZN and NSEG). Because PEN samples exhibit altered spectral features upon addition of BZN and NSEG, radiative energy transfer from the PEN matrix to the BZN or NSEG quencher might be occurring. However, all fluorescence measurements were carried out with a front-face geometry, which should reduce the potential effect of radiative energy transfer. Also, the effect of radiative energy transfer is expected to be small in the case of BZN. This is due to the absence of red shift in the emission spectra of BZN-containing matrices, an effect opposite to what would be expected if BZN contributed strongly to the overall fluorescence (cf. the emission spectrum of polyBZN in Figure 2b).

Discussion

The different behaviors observed in Figure 5 for the three quenchers are now investigated in a more detailed manner. Special attention is devoted toward explaining why some $\tau_D/\langle\tau\rangle$ curves do exhibit a break point with quencher concentration (BZN and NSEG), when others do not (I-DMT). Energy migration followed by trapping has been the object of intense scrutiny. Several theories have been derived to account for it.[9−12] Usually the donor fluorescence decay $F_D(t)$ is found to be an expression given as

$$F_D(t) = e^{-t/\tau_D} G_{DT}(t) \qquad (6)$$

where τ_D is the donor lifetime, and $G_{DT}(t)$ is the survival probability of the donor undergoing energy migration and trapping. In 1982, Loring et al. carried out the mathematical treatment (referred to in the following discussion as LAF), which would yield $G_{DT}(t)$ for a

system where donors and traps are immobile and randomly distributed inside a solid matrix.[9] Zumofen et al. considered a process in which the energy migrates among fractal sites, so that $G_{DT}(t)$ depends on the fractal dimension ($\bar{d}$) of the medium where energy migration and trapping are taking place.[10] They find

$$G_{DT}(t) = \exp(-at^{\bar{d}/2} + bt^{\bar{d}}) \quad (7)$$

where a and b are two constants. As Zumofen et al., Byers et al. also used a stretched exponential for $G_{DT}(t)$ where the exponent α depends on time:[11]

$$G_{DT}(t) = \exp(A(t)t^{\alpha(t)}) \quad (8)$$

Mollay and Kauffmann recognized that chromophores attached onto polymers do not adopt a random configuration.[12] To account for the constraint imposed onto the chromophores by the polymer backbone, their treatment generates several polymer chains by Monte Carlo simulations, which are left to adopt random configurations. The processes of energy migration and trapping are then monitored among the chromophores either attached on or constituting the polymer.

In this study, the fluorescence decays are considered for quencher contents where no rise time is observed. Thus, the system under study deals with energy migration and trapping processes occurring inside a pool of GS naphthalene dimers. According to the assumptions on which the LAF model is based,[9] the LAF model was selected in an effort to describe in a more quantitative fashion the experimental observations reported in Figure 5. The LAF model was favored because it does not deal with fractal dimensions and time-dependent exponents, which are often more difficult to interpret conceptually.[10,11] Furthermore, the LAF model, although not as complete as Mollay and Kauffmann's model, is simple to implement computationally.[12] Also, it is worth noting that, when Mollay and Kauffmann's model was applied to solid PEN, the lifetime of the naphthalene monomer needed to be fixed at 3.3 ns in order to fit the fluorescence decays.[3] This is significantly shorter than the 12 ns lifetime expected for the naphthalene monomer in such a polymer matrix.[2,5]

The LAF model depends on five parameters, namely C_D and C_T, which are the reduced concentrations of the donors and traps, respectively, R_0^{DD} and R_0^{DT}, which are the Forster radii for energy transfer between donors, or between a donor and a trap, respectively, and τ_D, which is the donor lifetime. The number densities for the donors (ρ_D) and for the traps (ρ_T) can be calculated from the knowledge of C_D, C_T, R_0^{DD}, and R_0^{DT}. For a given set of C_D, C_T, R_0^{DD}, R_0^{DT}, and τ_D, the solution of the LAF model is obtained in the Laplace space and is backtranformed into the real space.[16] Poisson noise was added to the fluorescence decays, and they were fitted with three exponentials.[17] τ_D was taken to equal 26.5 ns, the lifetime of the excited naphthalene dimers in PEN.[2] For each simulated decay, the average decay time $\langle\tau\rangle$ was calculated, and the ratio $\tau_D/\langle\tau\rangle$ was plotted as a function of ρ_T. Simulations were carried out for reduced donor concentrations C_D ranging from 0.2 to 100. For each C_D, the ratio R_0^{DT}/R_0^{DD} was adjusted so that a reasonable quenching efficiency could be obtained for quencher densities ρ_T ranging from $0.02\rho_D$ to $0.10\rho_D$, a range which corresponds to the quencher densities used in our fluorescence experiments. A typical $\tau_D/\langle\tau\rangle$ versus ρ_T plot is shown in Figure 6 for C_D equal to 100. All simulations yielded trends similar to that shown in Figure 6. No break point was observed. These results indicate that the LAF model will describe our results qualitatively as long as the quencher content is below some given concentration at which the break point is observed.

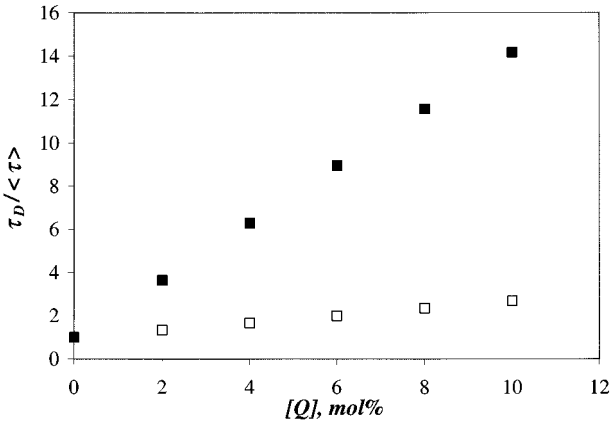

Figure 6. Plot of $\tau_D/\langle\tau\rangle$ as a function of quencher content. The fluorescence decays were simulated according to the LAF theory and fitted with a three-exponential fit. The parameters which were used were $C_D = 100$ and $R_0^{DT}/R_0^{DD} = 0.2$ for (■) and $C_D = 100$ and $R_0^{DT}/R_0^{DD} = 0.1$ for (□).

To explain the presence of a break point, we invoke a compartmentalization of the trapping process. Whether the excited quencher can fluoresce or not, it was first able to capture the energy migrating between naphthalene dimers. For each quencher, a capture volume V_C can be defined so that any energy migrating within V_C will be transferred to the quencher. Our V_C is somewhat similar to the surrounding sphere of action, which was introduced to handle static quenching cases.[8,18] When the quencher concentration is small, each quencher is isolated and covers a volume V_C. Within V_C, the quencher will exhibit its own response to the excitation from the PEN matrix. For I-DMT, a nonradiative relaxation occurs, whereas a radiative relaxation process will occur for BZN and NSEG. Since the quencher concentration is small, a large PEN volume is unoccupied by quenchers. Introducing additional quenchers generates additional V_C's, which leads to a linear increase of the quenching efficiency of a given quencher. As more quencher is added, a quencher content ($[Q]_{overlap}$) is reached where the entire PEN matrix is now covered by the quenchers. Any additional quencher will be located within an already existing V_C, where quenching is already taking place, and the quenching efficiency is expected to be less. This is clearly observed in Figure 5, where $\tau_D/\langle\tau\rangle$ increases much more slowly with quencher content after $[Q]_{overlap}$ has been reached. According to this explanation, the contents of BZN and NSEG used in this study go beyond $[Q]_{overlap}$, whereas those of I-DMT are always lower than $[Q]_{overlap}$. Thus, the plots of $\tau_D/\langle\tau\rangle$ versus quencher concentration exhibit a break point for BZN and NSEG, opposite to what is observed for I-DMT.

To account for the capture volume, an attempt was made to apply a blob model approach to handle our experiments dealing with energy migration and trapping. Recently, the concept of blob has been successfully applied to interpret complex kinetics occurring in polymeric systems where the polymer backbone has been randomly labeled with pyrene.[19,20] In the present

Scheme 1. Blob Representation of the Polymer Matrix

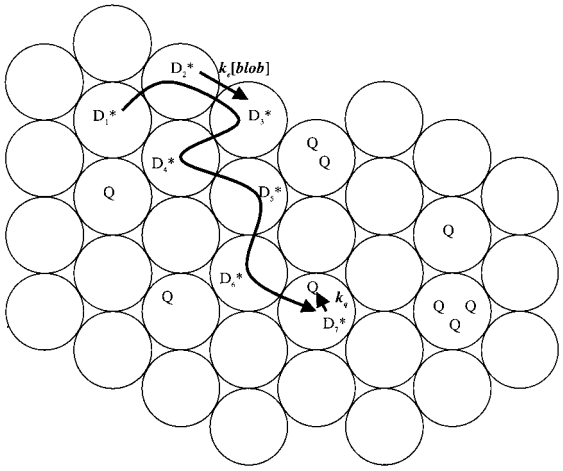

version of the blob model, the polymer matrix is divided into blobs, which are occupied by the quenchers. A blob is defined as $V_{blob} = V_C$, the volume within which quenching occurs with a rate constant k_q via energy transfer from a donor to a trap. The energy can migrate from one blob to the next with a rate constant k_e[blob] where k_e is the exchange rate constant and [blob] is the blob concentration inside the polymer matrix. $\langle n \rangle$ is the average number of traps per blob. Scheme 1 shows the blob representation of the polymer matrix.

According to the blob model, an expression for $G_{DT}(t)$ was derived in the Appendix and is given in eq 9.

$$G_{DT}(t) = \exp(-k_e[\text{blob}]t - \langle n \rangle(1 - \exp(-k_q t))) \quad (9)$$

Since the quenchers do not cover the entire polymeric matrix at low quencher concentration, some zones of the polymer matrix are expected to remain unquenched. This is taken into account by adding an extra exponential to yield eq 10:

$$F_D(t) = [D^*_Q]_{(t=0)} \times \exp(-t/\tau_D) \times G_{DT}(t) + [D^*_{NQ}]_{(t=0)} \times exp(-t/\tau_D) \quad (10)$$

where $[D^*_Q]_{(t=0)}$ and $[D^*_{NQ}]_{(t=0)}$ represent the donor concentrations at time $t = 0$ in domains with and without quencher, respectively, and $G_{DT}(t)$ is given by eq 9.

Although some of the quenchers are expected to emit some intrinsic fluorescence, all fluorescence decays for I-DMT and BZN were fitted with eq 10, which does not take into account any emission from the quenchers. Equation 10 is expected to hold for I-DMT regardless of I-DMT content because I-DMT does not seem to fluoresce. In the case of BZN, only those decays obtained with very low BZN contents (<3 mol %) are expected to exhibit little BZN fluorescence. For NSEG, a significant shift of the steady-state fluorescence spectrum is observed even with an NSEG content as low as 1 mol %. Thus, NSEG emission is certainly present in all our fluorescence decays dealing with this quencher, and these decays were not fitted with eq 10. Equation 10 was convoluted with the instrument response function, and the preexponential factors and the parameters k_q, k_e[blob], and $\langle n \rangle$ were recovered from the least-squares fitting analysis. Their values for I-DMT and BZN are listed in Table 2 along with the χ^2 parameters.

Table 2. Parameters Recovered from the Blob Model Analysis of the Fluorescence Decays (λ_{ex} = 350 nm and λ_{em} = 480 nm) of PEN Matrices Containing I-DMT and BZN and Using Eq 10

[Q], mol %	$\langle n \rangle$	k_q, 10^7 s^{-1}	k_e[blob], 10^7 s^{-1}	f_Q	χ^2
PEN Containing I-DMT					
2	0.21	6.1	2.5	0.25	1.37
3	0.24	8.0	1.5	0.17	1.62
4	0.37	8.4	2.3	0.19	1.15
5	0.33	11.7	3.1	0.20	1.06
7	0.78	7.5	1.7	0.04	1.24
PEN Containing BZN					
1	0.38	10	2.3	0.21	1.09
2	0.63	12	2.3	0.14	1.21
3	0.85	8	1.4	0.02	1.21
4	0.82	18	3.4	0.08	1.31
5	0.92	14	3.2	0.08	1.16
10	1.1	16	3.9	0.05	1.40

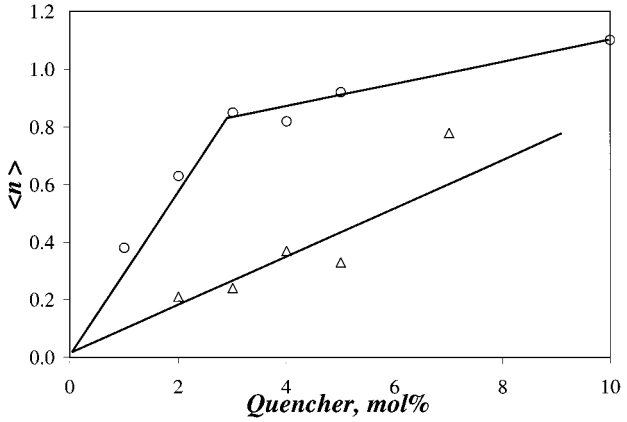

Figure 7. Plot of $\langle n \rangle$, the average number of quencher per blob, versus the quencher content. The different quencher types are I-DMT (△ in PEN) and BZN (○ in PEN).

It was found that, within experimental error, k_q remained constant with quencher content and equalled $(7.5 \pm 1.0) \times 10^7$ and $(13 \pm 4.0) \times 10^7$ s^{-1} for I-DMT and BZN, respectively. A plot of $\langle n \rangle$ versus quencher content is given in Figure 7. Figure 7 mimics what was observed in Figure 5. For I-DMT, $\langle n \rangle$ increases linearly with quencher content, whereas a clear break point is observed for BZN. Within the framework of the blob model, $\langle n \rangle$ is related to the volume of a blob. By definition, $\langle n \rangle$ is the average number of quenchers per blob. Thus eq 11 is obtained:

$$\frac{\langle n \rangle}{V_{blob}} = [Q]_{eff} \quad (11)$$

where V_{blob} is the volume of one blob and $[Q]_{eff}$ is the effective quencher concentration inside the polymer matrix. $[Q]_{eff}$ is larger than [Q], the average quencher concentration in the polymer matrix, because some zones of the polymer matrix are not quenched, when the quencher content is low. This led us to introduce the component $[D^*_{NQ}]_{(t=0)}$ in eq 10. Thus, in eq 10, $[D^*_Q]_{(t=0)}$ and $[D^*_{NQ}]_{(t=0)}$ give the fraction of excited naphthalene dimers that are in a quencher occupied domain and in a quencher-free domain, respectively. The effective quencher concentration is given by eq 12:

$$[Q]_{eff} = \frac{\langle n \rangle}{V_{blob}} = \frac{[Q]}{f_Q} \times 0.055 \text{ mol/L} \quad (12)$$

where $f_Q = [D^*_Q]_{(t=0)}/([D^*_Q]_{(t=0)} + [D^*_{NQ}]_{(t=0)})$ and [Q] is

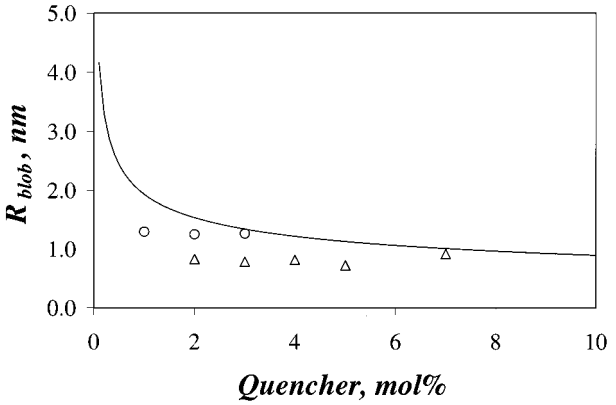

Figure 8. Plot of the blob radius as a function of quencher content. The different quencher types are I-DMT (△ in PEN) and BZN (○ in PEN). The solid line indicates the radius of the volume of the polymeric matrix available per quencher at a given quencher content.

Table 3. k_q, k_e[blob], and R_{blob} Values Obtained for BZN for Quencher Concentrations Smaller Than or Equal to 3 mol % (When R_{blob}(BZN) Intercepts the Solid Line in Figure 8) and I-DMT (for the Entire Quencher Concentration Range)

Q	k_q, 10^7 s^{-1}	k_e[blob], 10^7 s^{-1}	R_{blob}, nm
I-DMT	7.5 ± 1	2.0 ± 0.5	0.8 ± 0.1
BZN	10 ± 2	2.0 ± 0.5	1.3 ± 0.0

the average quencher concentration given in mol %. 0.055 mol/L is the equivalent concentration of 1 mol % quencher in PEN, and it was assumed to remain unchanged upon quencher addition to the PEN matrix. Equation 12 yields a relationship between V_{blob} and $\langle n \rangle$, [Q], and f_Q. Assuming spherical blobs, the blob radius is obtained as

$$R_{blob} = \left(\frac{3}{4\pi} \frac{10^{24}}{N_A} f_Q \frac{\langle n \rangle}{0.055[Q]} \right)^{1/3} \text{(nm)} \qquad (13)$$

where N_A is the Avogadro number. R_{blob} was plotted as a function of quencher content in Figure 8. In Figure 8, the solid line represents the radius of the polymer matrix volume available per quencher at a given quencher content. When for a given quencher content R_{blob} has a value located at or above the solid line, it indicates that the quenchers cover the entire polymer matrix. For R_{blob} located below the solid line, each added quencher is efficient and has a good probability of covering a zone deprived of quencher. As R_{blob} reaches or crosses the solid line in Figure 8, the quenchers now cover the entire polymer matrix, the quencher concentration equals $[Q]_{overlap}$, and further addition of quencher results in a less efficient quenching, because this domain of the polymer matrix is already being quenched. This saturation effect leads to the trend shown in Figure 5, namely the two break points observed for BZN and NSEG.

Table 3 summarizes the k_q, k_e[blob], and R_{blob} values obtained for BZN for quencher contents smaller than or equal to 3 mol % (BZN contents low enough so that BZN potential emission is small) and I-DMT (for the entire quencher concentration range). It is worth noting that the R_{blob} values, which were retrieved from the blob model analysis, are typical of Forster radii obtained for energy-transfer experiments.[21] According to Table 3, R_{blob}(BZN) and k_q(BZN) are larger than R_{blob}(I-DMT) and k_q(I-DMT). This conclusion correlates very well with the quenching efficiency of these compounds as shown in eq 5. If the data dealing with NSEG had been investigated with the blob model, a R_{blob}(NSEG) value larger than R_{blob}(BZN) would have been expected, since NSEG appears to be the best quencher.

Equation 13 can be used in order to determine the overlap concentration of I-DMT and BZN. The overlap concentration is reached when each blob contains in average one quencher or when $\langle n \rangle$ equals 1.0. The blob model predicts that the expression of the overlap concentration is given by eq 14.

$$[Q]_{overlap} = \frac{3}{4\pi} \frac{10^{24}}{N_A} \frac{1}{0.055 R_{blob}{}^3} \qquad (14)$$

Using the values of R_{blob} listed in Table 3, one finds that $[Q]_{overlap}$ equals 14 and 3.3 mol % for I-DMT and BZN, respectively. Since all quencher contents used in the study of I-DMT in a PEN matrix were below 14 mol %, a plot of $\tau_D/\langle\tau\rangle$ versus quencher content yields no break point, as observed experimentally. On the other hand, a break point would be expected for BZN for a quencher content of 3.3 mol %. It does indeed occur in Figure 5 at a slightly lower quencher content of 2 mol %.

Conclusion

The efficiency of three quenchers, I-DMT, BZN, and NSEG, at quenching the inherent fluorescence of PEN was investigated by steady-state and time-resolved fluorescence. It was found that NSEG is a better quencher than BZN, itself a better quencher than I-DMT. A quencher has the maximum impact at low quencher contents, because any added quencher covers a virgin polymer domain. As more quencher is added, the whole polymer matrix is covered, and any additional quencher occupies a polymer domain which is already quenched. Thus, its quenching efficiency is reduced, because it quenches an area which is already being quenched. This effect results in a break point observed in the plot of $\tau_D/\langle\tau\rangle$ versus quencher content for BZN and NSEG in Figure 5.

The saturation effect was further investigated by using a blob model. According to the blob model, quenching occurs inside a blob of radius R_{blob} with a quenching rate constant k_q. A more efficient quenching occurs for larger R_{blob} and k_q values. This is indeed observed. Analysis of the fluorescence decays using the blob model yields R_{blob} and k_q values of 0.8 ± 0.1 nm and (7.5 ± 1) × 10^7 s^{-1} for I-DMT and 1.3 ± 0.0 nm and (10 ± 2) × 10^7 s^{-1} for BZN. The fluorescence decays obtained for PEN matrices containing the quencher NSEG could not be studied with the blob model due to NSEG intrinsic fluorescence.

The process of energy migration inside the polymer matrix helps quench PEN fluorescence. The excitation will travel until it penetrates a domain, which contains a quencher. This results in an increased quenching efficiency, when it is compared to that of a quencher in a polymer matrix where no energy migration is taking place.

Finally, it is worth noting that eq 10 is usually available in standard fluorescence decay analysis packages so that the blob model analysis can be easily implemented in other laboratories.

Appendix

After excitation of the polymer matrix, the energy migrates among naphthalene dimers (the donors) until

trapping occurs. According to Scheme 1, the polymer matrix is divided into blobs. If i quenchers are located inside a blob, the migrating energy is transferred to the quenchers with a rate constant ik_q. k_q is the rate constant at which energy is transferred from an excited donor to a quencher located in a blob containing a single quencher. The migrating energy can hop from blob to blob with an exchange rate constant k_e. The donor natural fluorescence is characterized by the rate constant $k_f = 1/\tau_D$. If P_n represents a blob containing n quenchers, the kinetics of the blob model can be taken into account according to the three following equations:

$$\text{fluorescence: } P_n^* \rightarrow P_n; \qquad k_f[P_n^*] \qquad \text{(A-1a)}$$

$$\text{exchange: } P_n^* + P_j \rightarrow P_n + P_j^*; \quad k_e[P_n^*][P_j] \qquad \text{(A-1b)}$$

$$\text{quenching: } P_n^* \rightarrow P_n; \qquad nk_q[P_n^*] \qquad \text{(A-1c)}$$

These equations are adapted from those that were derived for micellar systems. According to the classic mathematical derivation of Tachiya,[22] one obtains eq A-2 as the time-dependent concentration profile of the excited donor disappearing via quenching.

$$[D^*](t) = \exp(-(k_f + k_e[\text{blob}])t - \langle n\rangle(1 - \exp(-k_q t))) \qquad \text{(A-2)}$$

Equation A-2 is the same as eq 9, except that eq 9 deals with infinitely long-lived excited donors (D*).

References and Notes

(1) Jones, A. S.; Dickson, T. J.; Wilson, B. E.; Duhamel, J.; Winnik, M. A. *Polym. Prepr.* **1996**, *37*, 229−230.

(2) Jones, A. S.; Dickson, T. J.; Wilson, B. E.; Duhamel, J. *Macromolecules* **1999**, *32*, 2956−2961.

(3) Spies, C.; Gehrke, R. *Macromolecules* **1997**, *30*, 1701−1710.

(4) Phillips, D. H.; Schug, J. C. *J. Chem. Phys.* **1969**, *50*, 3297−3306.

(5) Spies, C.; Gehrke, R. *Macromolecules* **1999**, *32*, 8383−8387.

(6) Stryer, L. In *Biochemistry;* W. H. Freeman and Co.: New York, 1995; Chapter 26.

(7) Ng, D.; Guillet, J. E. *Macromolecules* **1982**, *15*, 728−732.

(8) Lakowicz, J. R. In *Principles of Fluorescence Spectroscopy*; Plenum Press: New York, 1986.

(9) Loring, R. F.; Andersen, H. C.; Fayer, M. D. *J. Chem. Phys.* **1982**, *76*, 2015−2027.

(10) Klafter, J.; Blumen, A. *J. Chem. Phys.* **1984**, *80*, 875−877.

(11) Byers, J. D.; Friedrichs, M. S.; Friesner, R. A.; Webber, S. E. *Macromolecules* **1988**, *21*, 3402−3413.

(12) Mollay, B.; Kauffmann, H. F. *Macromolecules* **1994**, *27*, 5129−5140.

(13) Förster, Th. *Ann. Phys.* (*Leipzig*) **1948**, *2*, 55−75.

(14) Demas, J. N. In *Excited-State Lifetime Measurements*; Academic Press: New York, 1983; p 147.

(15) Press, W. H.; Flannery, B. P.; Teukolsky, S. A.; Vetterling, W. T. In *Numerical Recipes. The Art of Scientific Computing* (*Fortran Version*); Cambridge University Press: New York, 1992.

(16) Stehfest, H. *Comm. ACM* **1970**, *13*, 47−49. Stehfest, H. *Comm. ACM* **1970**, *13*, 624.

(17) Duhamel, J.; Yekta, A.; Ni, S.; Khaykin, Y.; Winnik, M. A. *Macromolecules* **1993**, *26*, 6255−6260.

(18) Frank, I. M.; Vavilov, S. I. *Z. Phys.* **1931**, *69*, 100−110.

(19) Vangani, V.; Duhamel, J.; Nemeth, S.; Jao, T.-C. *Macromolecules* **1999**, *32*, 2845−2854.

(20) Mathew, A. K.; Siu, H.; Duhamel, J. *Macromolecules* **1999**, *32*, 7100−7108.

(21) Berlman, I. B. In *Energy Transfer Parameters of Aromatic Compounds*; Academic Press: New York, 1973.

(22) Tachiya, M. *Chem. Phys. Lett.* **1975**, *33*, 289−292.

MA0005419